

Supramolecular Recognition. Terpyridyl Palladium and Platinum Molecular Clefs and Their Association with Planar Platinum Complexes

Andrew J. Goshe, Ian M. Steele, and B. Bosnich*

Contribution from the Department of Chemistry, The University of Chicago, 5735 South Ellis Avenue, Chicago, Illinois 60637

Received October 11, 2002; E-mail: bos5@uchicago.edu

Abstract: Molecular receptors, consisting of either two parallel cofacially disposed terpyridyl-Pd-Cl⁺ or terpyridyl-Pt-Cl⁺ units, are described. Concerted rotation of these units about the molecular spacer can alter their separation between 6.4 and 7.2 Å to accommodate the dimensions of molecular guests. Neutral and anionic planar complexes of platinum(II) were investigated as guests to determine if metal-metal interaction between the host and guest metals could stabilize host-guest association. With a neutral guest, it was found that host-guest formation is signaled by a color change from light yellow to deep red. For one of the anionic guests, a visible absorption band appears upon host-guest formation with the platinum receptor that is ascribed to transitions associated with a Pt-Pt interaction. The association constants found for the neutral guest with the palladium and platinum receptors are large, suggesting that metal-metal interaction contributes to the molecular recognition. The structures of the host-(neutral)guest complexes in solution have been determined by ¹H NOESY spectra. A crystal structure of the platinum host-(neutral)guest complex is the same as that found in solution and confirms the presence of a Pt-Pt interaction. Temperature-dependent ¹⁹⁵Pt NMR spectra in solution provide a quantitative estimate of the conformational interconversions of the free platinum receptor.

Magnus' salt,¹ [Pt(NH₃)₄][PtCl₄], is green in the solid state despite the fact that the [Pt(NH₃)₄]²⁺ ion is colorless and [PtCl₄]²⁻ is pink in color. Its solid-state structure² consists of infinite alternating stacks of the dication and dianion with the platinum atoms aligned in a linear array separated by 3.23(2) Å. Solid-state spectroscopic studies reveal a strong electronic absorption band which is polarized along the stacked platinum atoms.³ A similar electronic absorption band is observed for the structurally analogous palladium double salt,⁴ but it is displaced to higher energies,³ and, as a consequence, the visible color of [Pd(NH₃)₄][PdCl₄] is reflected in the colors of the constituent ions. The particular stacking of the ions in Magnus' green salt may be largely controlled by electrostatic interactions, but such stacking has been observed for other platinum complexes that are anionic or cationic or neutral. Of special interest are the various salts of the colorless ion, [Pt(CN)₄]²⁻, which display a variety of colors in the solid state⁵ that depend on the Pt-Pt distances⁶ that range from 3.09 to 3.60 Å. As was noted,⁷ the shorter the Pt-Pt distance, the longer the wavelength

of the absorption band that is polarized along the Pt-Pt bonds in the solid state. Thus, Mg[Pt(CN)₄]·7H₂O (Pt-Pt, 3.16 Å; ν , 18 000 cm⁻¹) is red, Ba[Pt(CN)₂]·4H₂O (Pt-Pt, 3.32 Å; ν , 22 000 cm⁻¹) is yellow-green, and Ca[Pt(CN)₄]·5H₂O (Pt-Pt, 3.38 Å; ν , 22 800 cm⁻¹) is yellow.^{5,6} More recently, it was discovered that neutral 2,2'-dipyridyl or *o*-phenanthroline platinum(II) complexes form solid-state extended structures that have Pt-Pt distances in the range from 3.235 to 3.493 Å and have distinct colors in the solid state.⁸ Similarly, cationic 2,2':6',2''-terpyridine (terpy) platinum(II) complexes form extended solid-state structures having Pt-Pt distances of about 3.27 Å for the chloro complex.⁹ These studies have been extended to tethered cationic terpy platinum complexes which exist as dimers and trimers in solutions and in the solid state.¹⁰

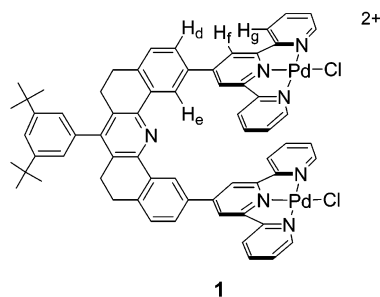
As noted, in the case of Magnus' double salt, the structure is likely to be determined by electrostatic interaction, whereas for

- (1) Magnus, G. *Ann. Phys. Chem.* **1828**, *14*, 239–242.
- (2) Atoji, M.; Richardson, J. W.; Rundle, R. E. *J. Am. Chem. Soc.* **1957**, *79*, 3017–3020.
- (3) Anex, B. G.; Takeuchi, N. *J. Am. Chem. Soc.* **1974**, *96*, 4411–4416. Anex, B. G.; Foster, S. I.; Fucaloro, A. F. *Chem. Phys. Lett.* **1973**, *18*, 126–128. Rodgers, M. L.; Martin, D. S. *Polyhedron* **1987**, *6*, 225–254. Miller, J. R. *J. Chem. Soc.* **1961**, 4452–4457. Miller, J. S. *Extended Linear Chain Compounds*; Plenum: New York, 1982–1983; Vols. 1–3.
- (4) Miller, J. R. *J. Chem. Soc.* **1965**, 713–720.
- (5) Gliemann, G.; Yersin, H. *Struct. Bonding* **1985**, *62*, 87–153.
- (6) Krogmann, K. *Angew. Chem., Int. Ed. Engl.* **1969**, *8*, 35–42.

- (7) Yamada, S.; Tsuchida, R. *J. Am. Chem. Soc.* **1953**, *75*, 6351–6352. Yamada, S. *Bull. Chem. Soc. Jpn.* **1951**, *24*, 125–127. Yamada, S. *J. Am. Chem. Soc.* **1951**, *73*, 1579–1580. Yamada, S. *J. Am. Chem. Soc.* **1951**, *73*, 1182–1184. Yamada, S.; Tsuchida, R. *Bull. Chem. Soc. Jpn.* **1949**, *70*, 142–144.
- (8) Connick, W. B.; Marsh, R. E.; Schaefer, W. P.; Gray, H. B. *Inorg. Chem.* **1997**, *36*, 913–922. Connick, W. B.; Henling, L. M.; Marsh, R. E.; Gray, H. B. *Inorg. Chem.* **1996**, *35*, 6261–6265.
- (9) Bailey, J. A.; Hill, M. G.; Marsh, R. E.; Miskowski, V. M.; Schaefer, W. P.; Gray, H. B. *Inorg. Chem.* **1995**, *34*, 4591–4599. Bailey, J. A.; Miskowski, V. M.; Gray, H. B. *Inorg. Chem.* **1993**, *32*, 369–370. Hill, M. G.; Bailey, J. A.; Miskowski, V. M.; Gray, H. B. *Inorg. Chem.* **1996**, *35*, 4585–4590.
- (10) Lai, S.-W.; Lam, H.-W.; Lu, W.; Cheung, K.-K.; Che, C.-M. *Organometallics* **2002**, *21*, 226–234. Lu, W.; Zhu, N.; Che, C.-M. *J. Chem. Soc., Chem. Commun.* **2002**, 900–901.

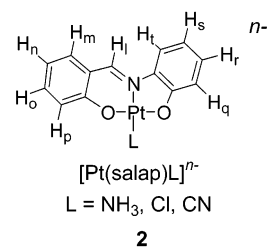
neutral dipyriddy and phenanthroline platinum complexes, π - π stacking and metal-metal interactions are probably the major forces that determine these structures.⁸ Significant stability contribution to the structure from metal-metal interactions is likely to be present only when the Pt-Pt distance is less than 3.5 Å. Although π - π and metal-metal interactions are weak, they become substantial by the cumulative effects of crystal packing. The stability of metal-metal interactions in crystals of ions of like charge, such as $[\text{Pt}(\text{CN})_4]^{2-}$ and $[\text{terpy-Pt-X}]^+$, may arise from the ability of the counterions to neutralize the strong electrostatic repulsions that exist between the like charged ions. These observations of Pt-Pt interactions in the solid state have prompted us to entertain the prospect of devising a soluble, medium molecular weight system that would lead to the molecular recognition of planar platinum(II) complexes by means of weak Pt-Pt interactions.

We recently described the molecular recognition displayed by the receptor molecule, **1**, $[\text{L}_R\text{Pd}_2\text{Cl}_2]^{2+}$.¹¹⁻¹⁴ The dicationic receptor, **1**, has coparallel terpy-Pd-Cl⁺ units constrained by the spacer fragment. The maximum separation of the two terpy-Pd-Cl⁺ units is about 7.2 Å, but by concerted rotation of the terpy-Pd-Cl⁺ units in relation to the spacer, the separation can be reduced to about 6.4 Å while essentially retaining the eclipsed disposition of the two terpy-Pd-Cl⁺ units. This flexibility of aperture of the molecular cleft in **1** allows the receptor to match the "thickness" of the incarcerated guest. The receptor, **1**,¹³ and its supramolecular derivatives¹² form host-guest complexes with a variety of planar aromatic molecules. The guest, 9-methylanthracene (9-MA), forms a stable 2:1 complex where one 9-MA guest resides inside of the cleft and the other lies on the outside face of one of the terpy-Pd-Cl⁺ units. Although stable, these host-guest complexes are exceedingly labile¹⁴ at room temperature where both rapid intra- and intermolecular exchange occurs. It is supposed that the stability of host-guest complexes is controlled by π - π interactions and possibly by charge-induced dipole attractive forces.¹⁴ The receptor, **1**, and its platinum(II) analogue, however, embody additional elements which could serve as forces in molecular recognition. These receptors are positively charged and hence are expected to be powerful receptors for negatively charged guests having dimensions compatible with the dimensions of the molecular cleft. Given the close association of the host and guest, and the low dielectric constant within the cleft, attractive electrostatic interactions are expected to be large.^{13,14} The flexible separation of the two metals of the two terpy-M-Cl⁺ units of the receptors is ideally suited for incarcerating a planar platinum(II) compound in an orientation which allows for stabilizing M-Pt-M interactions. In some respects, such a host-guest complex with the M-Pt-M interactions can be regarded as a fragment of the extended stacked structures observed in crystals. An exploration of these two stabilizing interactions with the palladium and platinum receptors is the subject of this paper.



Synthesis

Before the synthesis of the platinum(II) guest and receptor is described, a number of observations relevant to the selection of the guest molecules are provided. Addition of $[(\text{terpy})-\text{M}-\text{Cl}]^+$, $\text{M} = \text{Pd}^{2+}$, Pt^{2+} , to acetonitrile solutions of the Pd^{2+} or Pt^{2+} receptors of the type **1** does not lead to any association as judged by ¹H NMR chemical shifts or changes in color. Thus, it appears that whatever stabilization may accrue from π - π interactions and trimetal interactions by association of the $[(\text{terpy})-\text{M}-\text{Cl}]^+$ guest in the cleft is overcome by electrostatic repulsion between the positively charged receptor and guest. Addition of a methanol solution of $\text{K}_2[\text{Pt}(\text{CN})_4]$ to acetonitrile or DMF solutions of either the Pd^{2+} or the Pt^{2+} receptor leads to immediate precipitation of a very insoluble, gelatinous solid which, after heating of the mixture, transforms to a red, insoluble powder. Presumably, in these cases, host-guest association occurs, but the insolubility of the products precluded further studies. Similar insoluble precipitates are formed when the bis-oxalate complex, $\text{K}_2[\text{Pt}(\text{ox})_2]$,¹⁵ is added to the receptors. Several other anionic platinum(II) complexes were also tried and gave similar insoluble products with the receptors. In an attempt to generate soluble host-guest complexes using the present receptors with anionic platinum(II) complexes as guests, it was supposed that monoanionic guests composed of large aromatic, unsymmetrical ligands might provide the desired solubility. Whereas these guests did give solutions which persisted long enough to carry out physical measurements, eventually precipitation occurred. The guests chosen are platinum(II) complexes incorporating the tridentate ligand, salap, and are of the type **2**.

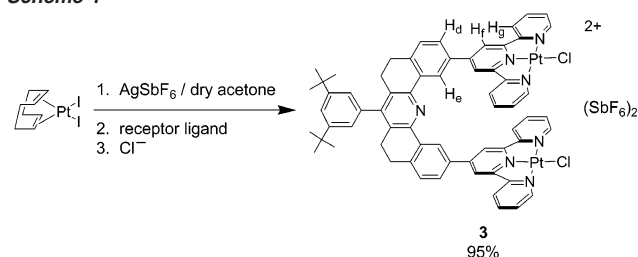


The $[\text{Pt}(\text{salap})\text{L}]^{n-}$ complexes were prepared in essentially quantitative yield by displacement of the dimethyl sulfoxide (DMSO) ligand from the known complex,¹⁶ $[\text{Pt}(\text{salap})\text{DMSO}]$. The anionic complexes were precipitated as their tetra-*n*-

- (11) Sommer, R. D.; Rheingold, A. L.; Goshe, A. J.; Bosnich, B. *J. Am. Chem. Soc.* **2001**, *123*, 3940-3952.
 (12) Goshe, A. J.; Bosnich, B. *Synlett* **2001**, 941-944.
 (13) Goshe, A. J.; Crowley, J. D.; Bosnich, B. *Helv. Chim. Acta* **2001**, *84*, 2971-2985.
 (14) Goshe, A. J.; Steele, I. M.; Ceccarelli, C.; Rheingold, A. L.; Bosnich, B. *Proc. Natl. Acad. Sci. U.S.A.* **2002**, *99*, 4823-4829.

- (15) Houlding, V. H.; Miskowski, V. M. *Coord. Chem. Rev.* **1991**, *111*, 145-152. Lee, K. H.; Kim, J. H.; Mizuno, M. *Bull. Korean Chem. Soc.* **1987**, *8*, 137-140. Mizuno, M. *Synth. Met.* **1987**, *19*, 963-966. Little, W. A.; Lorentz, R. *Inorg. Chim. Acta* **1976**, *18*, 273-278. Underhill, A. E.; Watkins, D. M.; Williams, J. M.; Carneiro, K. *Linear Chain Bis(oxalate)-palatinate Salts*. In *Extended Linear Chain Compounds*; Miller, J. S., Ed.; Plenum Press: New York, 1982; Vol. 1, pp 119-156.
 (16) Motschi, H.; Nussbaumer, C.; Pregosin, P. S.; Bachechi, F.; Mura, P.; Zambonelli, L. *Helv. Chim. Acta* **1980**, *63*, 2071-2086.

Scheme 1



butylammonium salts, which are soluble in polar organic solvents. The preparation of the palladium(II) receptor, **1**, as its PF_6^- salt has been described,¹¹ but the preparation of the platinum(II) analogue presented difficulties because of the kinetic inertness of the usual starting materials such as $[\text{PtCl}_4]^{2-}$. It was found that the yellow platinum(II) receptor could be prepared in high yield under mild conditions by the sequence outlined in Scheme 1. Two aspects of this reaction are crucial for its success. Anhydrous acetone is required throughout the reaction; otherwise, aquo complexes are formed with the intermediates. The displacement of the aquo ligands is slow, leading to impure products. The use of the SbF_6^- ion rather than PF_6^- leads to a purer product, probably because the cationic intermediates are capable of abstracting F^- ions from PF_6^- .

Host–Guest Formation with $[\text{Pt}(\text{salap})\text{NH}_3]$

When a yellow acetonitrile solution of $[\text{Pt}(\text{salap})\text{NH}_3]$ is added to acetonitrile solutions of the yellow palladium receptor, **1**, a deep orange-red color forms at once. Similarly, addition of $[\text{Pt}(\text{salap})\text{NH}_3]$ to an acetonitrile solution of the yellow platinum receptor **3**, $[\text{L}_R\text{Pt}_2\text{Cl}_2]^{2+}$, leads to the formation of an intensely colored dark red-brown solution. These observations indicate that host–guest complexes are formed.

The visible absorption spectrum for a 1:1 mixture of **3** and $[\text{Pt}(\text{salap})\text{NH}_3]$ is shown in Figure 1 together with the spectrum of the host and the guest and the sum of these spectra. The spectrum of the host–guest complex formed by **1** and $[\text{Pt}(\text{salap})\text{NH}_3]$ is given in the Supporting Information. Host–guest formation is signaled by new absorptions that are poorly resolved but whose presence is indicated by bands that are observed to lower energies of $20\,000\text{ cm}^{-1}$ where neither the host nor the guest absorb significantly. Such host–guest absorptions are usually referred to as charge transfer transitions, presumably involving electron transfer between the host and guest. Whereas transitions associated with the putative trimetal interactions in host–guest complexes involving the palladium receptor are not expected to occur in the visible region, such transitions could occur in this region with the host–guest complex formed by the platinum receptor, **3**. The host–guest spectrum shown in Figure 1 does not show a clearly defined band that could be assigned to transitions associated with trimetal interaction.

The stoichiometry and association constants for host–guest formation with the palladium, **1**(PF_6)₂, and platinum, **3**(SbF_6)₂, receptors and $[\text{Pt}(\text{salap})\text{NH}_3]$ in acetonitrile solutions at $70\text{ }^\circ\text{C}$ were determined by the mole ratio method¹⁷ using ^1H NMR spectroscopy chemical shifts. At lower temperatures, the ^1H NMR signals are broad for the two host–guest complexes but become sharp at the higher temperature. For both receptors, **1** and 0.1 mM concentrations of the receptors were used with the

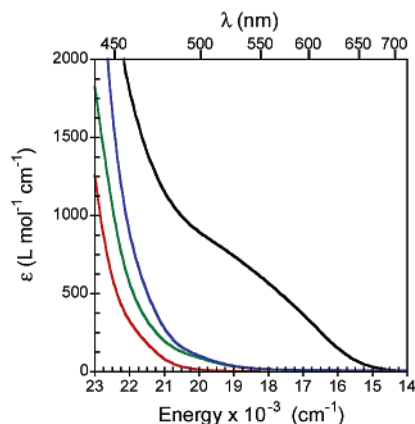


Figure 1. Absorption spectra for (green line) $[\text{L}_R\text{Pt}_2\text{Cl}_2](\text{SbF}_6)_2$ (1.96 mM), (red line) $[\text{Pt}(\text{salap})\text{NH}_3]$ (1.96 mM), (blue line) sum of the spectrum of $[\text{L}_R\text{Pt}_2\text{Cl}_2](\text{SbF}_6)_2$ and $[\text{Pt}(\text{salap})\text{NH}_3]$, and (black line) a 1:1 solution of **3** and $[\text{Pt}(\text{salap})\text{NH}_3]$ (1.96 mM each).

same result. Chemical shifts are observed for protons of the host and of the guest upon molecular association. Proton H_f (see **1** and **3**) provided the largest chemical shift, and these signals were monitored during the titration. From the plots of chemical shift versus guest concentration (see Supporting Information), a 1:1 stoichiometry for the host–guest complexes of both the palladium and the platinum receptors was unambiguously established. From these plots, it was found that the host–guest association constant for the palladium receptor was $12\,000 \pm 2900\text{ M}^{-1}$, and for the platinum receptor a value of $51\,000 \pm 8400\text{ M}^{-1}$ was determined. As compared with the first association constant found for the palladium receptor with 9-methylanthracene¹¹ of 600 M^{-1} , these constants are considerably larger, and the higher constants suggest that metal–metal bonding may contribute to the stability of the complexes formed with $[\text{Pt}(\text{salap})\text{NH}_3]$. This supposition is supported by the observation of a higher association constant for the platinum-based receptor, which would be expected to have stronger metal–metal interactions. In addition to these metal–metal interactions, stability to the association complexes is provided by π – π interactions and possibly by charge-induced dipole interactions that will exist between the complexed salap ligand and the terpy ligands.

The formation of 1:1 host–guest complexes suggests that the guest resides in the molecular cleft of the receptors, but the discovery that 9-methylanthracene can reside outside of the cleft as well as inside^{11,12,14} elicits caution. The most direct method of establishing the site residency of the guest is by ^1H NOESY experiments. These were carried out at $70\text{ }^\circ\text{C}$ in acetonitrile solutions using 1:1 concentrations of host and guest. Similar, but different, results were obtained for the palladium and platinum receptors. Figure 2 summarizes, using arrows to represent the cross-peaks, the NOE cross-peaks that were observed for the palladium receptor. In this case, only cross-peaks associated with the inner protons of the spacer, H_e , were observed. No cross-peaks with the outer spacer protons, H_d , were observed. These observations are consistent with the supposition that the guest resides in the molecular cleft and has no significant residency time positioned on the outer faces of the terpy–Pd– Cl^+ units as was observed with 9-methylanthracene. The existence of cross-peaks between the H_e protons and H_m , H_i , and H_t as well as H_p , H_k , and H_q , but not with the other aromatic

(17) Meyer, A. S., Jr.; Ayres, G. H. *J. Am. Chem. Soc.* **1957**, *79*, 49–53.

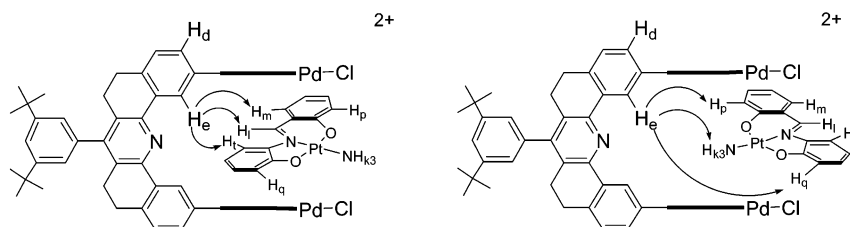


Figure 2. Intermolecular ^1H NOEs observed for a 1:1 CD_3CN solution of $[\text{L}_R\text{Pd}_2\text{Cl}_2](\text{PF}_6)_2$ and $[\text{Pt}(\text{salap})\text{NH}_3]$ at 70°C .

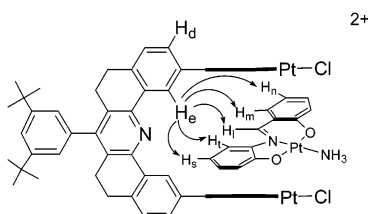


Figure 3. Intermolecular ^1H NOEs observed for a 1:1 CD_3CN solution of $[\text{L}_R\text{Pt}_2\text{Cl}_2](\text{SbF}_6)_2$ and $[\text{Pt}(\text{salap})\text{NH}_3]$ at 70°C .

protons of the salap ligand, indicates two aspects of the geometry of the guest in the cleft. First, these results suggest that the long axis of the $[\text{Pt}(\text{salap})\text{NH}_3]$ guest and the long axis of the terpy-Pd-Cl $^+$ units are aligned roughly parallel to each other. Second, within this coparallel orientation, the guest can exist in two orientations with respect to the spacer, one where the azamethine proton points at the spacer and the other where the ammine ligand is directed at the spacer. The ^1H NMR spectrum of this complex is consistent with the presence of a single host-guest complex, and, consequently, the two orientations of the guest are in rapid exchange. This exchange could occur either by rapid rotation of the guest about the putative metal-metal bonds or by intermolecular exchange. No evidence has been obtained which distinguishes these two possible mechanisms.

The NOESY cross-peaks observed for the platinum host-guest complex are represented using arrows in Figure 3. As for the palladium receptor, no cross-peaks are observed with the outer spacer proton, H_d , indicating that the guest lies in the cleft. The shown cross-peaks (Figure 3) indicated that, for the platinum receptor, the guest resides in only one orientation, with the azamethine proton, H_i , pointing at the spacer. It is not obvious that there are significant structural differences between the two receptors that might lead to the guest having two orientations in the palladium receptor but only one in the platinum host. It therefore seems that the difference is connected with the stronger metal-metal interaction that should exist in the platinum host. Perhaps in this case the stronger metal-metal interaction leads to smaller separation between the two terpy-Pt-Cl $^+$ units, which restricts the orientation of the guest by nonbonded interactions. That this assertion may have validity is supported by a crystal structure.

Crystal Structure

Dissolution of a 1:1 mixture of $[\text{Pt}(\text{salap})\text{NH}_3]$ and the platinum receptor, **3**, in propionitrile led to immediate host-guest formation. Vapor diffusion with methanol gave very small red needles of the host-guest adduct as the di-SbF $_6$ salt with one crystallization molecule of propionitrile. Synchrotron radiation (0.72588 \AA) was used to obtain crystal data; a summary of the refinement data and other information is provided in Table 1. Three perspectives of the host-guest complex are illustrated

Table 1. Crystallographic Data for $3\cdot[\text{Pt}(\text{salap})\text{NH}_3](\text{SbF}_6)_2\cdot\text{CH}_3\text{CH}_2\text{CN}$

compound	$3\cdot[\text{Pt}(\text{salap})\text{NH}_3](\text{SbF}_6)_2\cdot\text{CH}_3\text{CH}_2\text{CN}$
formula	$\text{C}_{81}\text{H}_{72}\text{Cl}_2\text{F}_{12}\text{N}_{10}\text{O}_2\text{Pt}_3\text{Sb}_2$
formula weight	2345.16 (including solvent)
space group	$P\bar{1}$
a , \AA	10.500(2)
b , \AA	19.809(4)
c , \AA	21.842(4)
α , deg	98.52(3)
β , deg	96.69(3)
γ , deg	102.70(3)
V , \AA^3	4330.2(15)
Z , Z'	2
cryst. size, color, habit	$0.08 \times 0.005 \times 0.005$ mm, red, needle
$D(\text{calc})$, g cm^{-3}	1.799
μ , mm^{-1}	5.582
temp, K	110 K
wavelength	0.72588 \AA (synchrotron radiation)
$R(F)$, % a	5.56
$R(wF^2)$, % a	14.55

a Quantity minimized = $R(wF^2) = \frac{\sum[w(F_o^2 - F_c^2)^2]}{\sum[(wF_o^2)^2]^{1/2}}$; $R = \frac{\sum\Delta}{\sum(F_o)}$, $\Delta = |F_o - F_c|$; $w = 1/[\sigma^2(F_o^2) + (aP)^2 + bP]$, $P = [2F_c^2 + \max(F_o, 0)]/3$.

in Figure 4. The spacer is in a racemic conformation with the unit cell carrying the two enantiomers. The two terpy-Pt-Cl $^+$ units are twisted with respect to the spacer by about 42° , and the guest lies in the molecular cleft in the same orientation as was determined in solution. The bond lengths and angles of the receptor and of the guest are unexceptional, and the crystallographic data are provided in the Supporting Information as a CIF file. The Pt-Pt distances are Pt(1)-Pt(3), 3.303 \AA and Pt(2)-Pt(3), 3.262 \AA . The three platinum atoms are not perfectly aligned: Pt(1) is displaced from Pt(3) by 0.36 \AA in the direction of N(1), while Pt(2) is displaced from Pt(3) by 0.50 \AA in the direction of N(7). These small displacements probably arise from the twisting of the terpy-Pt-Cl $^+$ units. The platinum atom (Pt(3)) of the guest is essentially aligned with the two host platinum atoms with respect to the other planar perpendicular axis; the displacement of Pt(3) from the line joining Pt(1) and Pt(2) away from the spacer is 0.2 \AA . The short Pt-Pt distances indicate that tri-platinum bonding occurs in the host-guest complex. Such a Pt-Pt interaction does not extend beyond the host-guest unit in the extended crystal structure. As illustrated in Figure 5, the neighboring terpy-Pt-Cl $^+$ units of different receptors have their platinum atoms displaced from each other leading to a metal-metal separation of 4.287 \AA , which is too large for any significant metal-metal bonding. The separations between the units and their interplanar angles are shown schematically in the Supporting Information. The terpy-Pt-Cl $^+$ units and the guest are all nearly parallel to each other. The interplanar separation between terpy-Pt-Cl $^+$ units of different receptors is 3.442 \AA , a separation that is typical of π -stacked aromatic molecules. Presumably, such π - π interactions are responsible for the extended stacking of the receptor

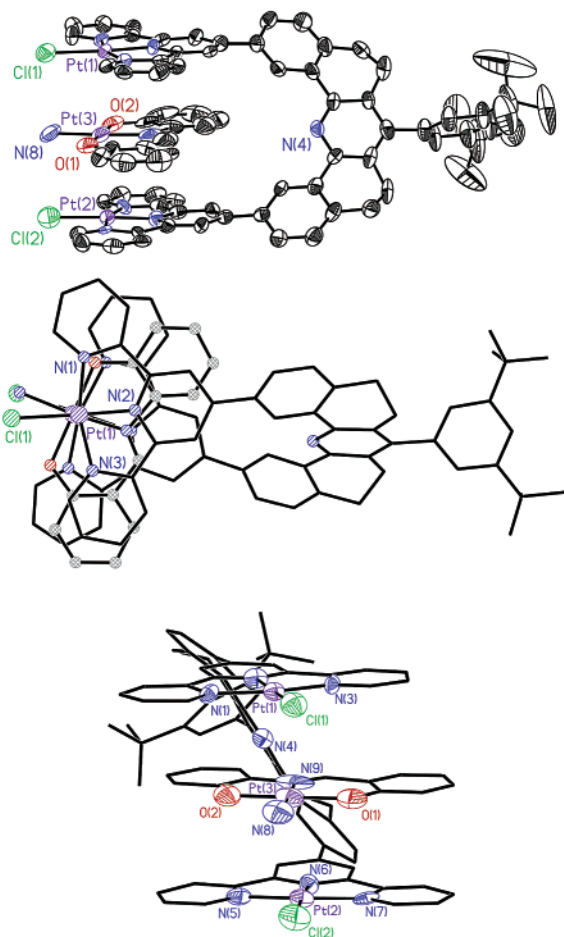


Figure 4. Three perspectives of the molecular adduct, $3 \cdot [\text{Pt}(\text{salap})\text{NH}_3] \cdot (\text{SbF}_6)_2 \cdot \text{CH}_3\text{CH}_2\text{CN}$, a “side” view, a “top” view, and a “front” view. Solvent molecules and counterions have been removed for clarity. Thermal ellipsoids are shown at the 50% probability level.

terpy–Pt–Cl⁺ units in the crystal (Figure 5). The separation between the terpy–Pt–Cl⁺ units and the guest in the cleft (3.286 and 3.271 Å) is considerably less than that expected for simple π – π stacking. The same separations for the host–guest complex formed between **1** and 9-methylanthracene were found to be 3.44 and 3.48 Å.¹¹ It seems reasonable to conclude that the short separation observed between the terpy–Pt–Cl⁺ units and the [Pt(salap)NH₃] guest is because of metal–metal bonding in the host–guest complex. This metal–metal interaction thus represents a previously unexplored force in molecular recognition, and the host–guest unit may be regarded as a soluble fragment of the extended metal–metal interactions observed in crystals.

Cation–Anion Host–Guest Interactions and Electronic Spectra

The yellow palladium receptor, **1**, and the platinum receptor, **3**, as 10^{-3} M solutions in acetonitrile or DMF at 20 °C form association complexes with 1 equiv of the light yellow anionic guests, *n*-Bu₄N[Pt(salap)CN] and *n*-Bu₄N[Pt(salap)Cl], as evidenced by the formation of deep red colored solutions. Many of these solutions become viscous over time and eventually deposit crystals. The ¹H NMR spectra of all of these host–guest solutions are very broad at 20 °C and remain so up to 70 °C, suggesting that extensive association occurs between the species in solution. The slow formation of gels for some of these

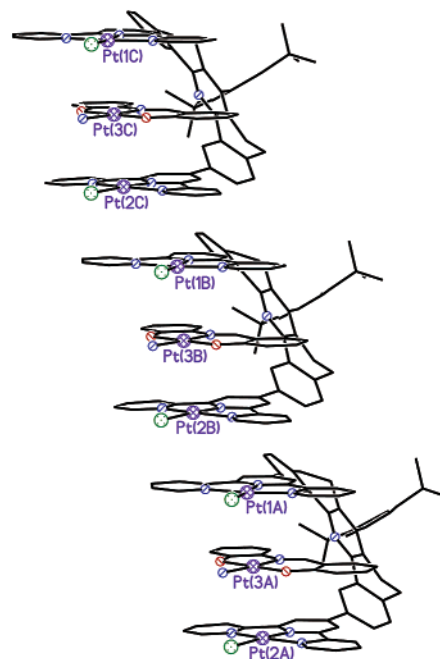


Figure 5. An illustration of the stacking present in crystals of $3 \cdot [\text{Pt}(\text{salap})\text{NH}_3] \cdot (\text{SbF}_6)_2 \cdot \text{CH}_3\text{CH}_2\text{CN}$. Solvent molecules and counterions have been removed for clarity.

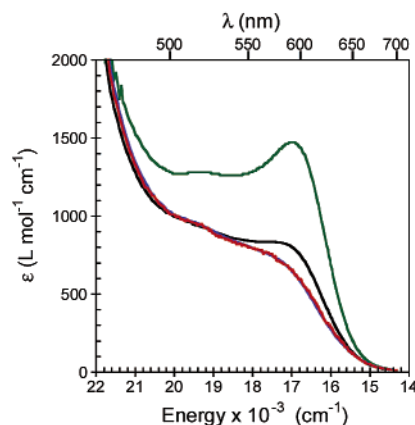


Figure 6. The concentration dependence of the absorption spectra for a 1:1 solution of [L_RPt₂Cl₂](SbF₆)₂ and *n*-Bu₄N[Pt(salap)CN] in DMF (green line) 1.00×10^{-2} M, (black line) 1.00×10^{-3} M, (blue line) 1.00×10^{-4} M, and (red line) 1.00×10^{-5} M; the last two spectra are identical.

solutions supports the assertion that extensive association exists. The nature of these solutions and the solids which precipitate from them will be reported elsewhere, but the electronic absorption spectra observed for the platinum receptor, **3**, and the anionic guest, [Pt(salap)CN][−], are germane to the present study.

Addition of 1 equiv of *n*-Bu₄N[Pt(salap)CN] to a 10^{-3} M solution of the platinum receptor, **3**, in acetonitrile or DMF leads to the immediate formation of deep red solutions which have similar visible absorption spectra. After about 15 min, the acetonitrile solution becomes a viscous gel, but the corresponding DMF solution remains mobile. The visible absorption spectra of equivalent concentrations of receptor, **3**, and the anionic cyano complex guest in DMF solution are shown in Figure 6 for concentrations between 10^{-2} to 10^{-5} M. The spectra for 10^{-4} and 10^{-5} M are identical, but at higher concentrations the spectra are different in both intensity and form.

Because it is highly probable that 1 equiv of the guest resides exclusively in the molecular cleft of the receptors as was shown for the ammine guest, the concentration behavior of the spectra indicates that, at the higher concentrations, there is association of the host–guest complexes. At concentrations lower than 10^{-4} M, the dissociation between host–guest complexes appears to be complete. The most likely form of solution stacking of the host–guest molecules is that resembling the extended solid-state structure shown in Figure 5 for the ammine guest.

The absorptions observed to lower energies of $20\,000\text{ cm}^{-1}$ are those associated with host–guest formation because the constituent parts do not have absorption in this region. Unlike the spectra of the host–guest complex formed by **3** and [Pt(salap)NH₃] (Figure 1), the present host–guest complex shows two broad absorption manifolds, one at about $19\,500\text{ cm}^{-1}$ and the other at about $16\,500\text{ cm}^{-1}$. The higher energy band, at $19\,500\text{ cm}^{-1}$, occurs at about the same energy as that of the host–guest complex formed between **3** and [Pt(salap)NH₃] (Figure 1). The lower energy band is distinct and is ascribed to transitions associated with Pt–Pt interactions. The concentration dependence of this lower energy band suggests that its electronic provenance is not only connected with a Pt–Pt interaction of the host–guest complex but also with Pt–Pt interactions which occur because of stacking of the outer faces of the terpy–Pt–Cl⁺ units of neighboring receptors. That such stacking does not appear to occur between the host–guest complexes formed by **3** and [Pt(salap)NH₃] is probably related to the lower net positive charge that exists for the host–guest complex formed between **3** and the anionic cyano guest.

Clearly complicated association phenomena exist in solutions of host–guest complexes formed with anionic guests, a circumstance which may explain the absence of sharp ¹H NMR spectra for such solutions. It also appears that for 10^{-3} M or greater concentrations, solutions of these host–guest complexes are kinetically preserved because eventually precipitation of the host–guest complexes occurs. The rate of precipitation increases with increase in temperature.

¹⁹⁵Pt NMR Spectra

The ¹⁹⁵Pt NMR spectra of the receptor, **3**, the free guest, [Pt(salap)NH₃], and of the host–guest association complex formed by the two were measured in acetonitrile solutions using an aqueous solution of K₂[PtCl₆] as an external reference. A 400 MHz spectrometer was used, and the ¹⁹⁵Pt signals were found to be broad, probably due to ¹⁴N, ³⁵Cl, and ³⁷Cl nuclear spin interactions.¹⁸ The broadness of the signals precluded observation of any Pt–Pt coupling in the host–guest complex, but because of the large chemical shifts of the ¹⁹⁵Pt nuclei, it was possible to follow, what is assumed to be, the racemic–meso interconversion in the free receptor, **3**.

At 20 °C and below, the free receptor, **3**, displays two ¹⁹⁵Pt NMR signals, one at $-2715\text{ }\delta$ and the other at $-2734\text{ }\delta$. These two signals are assigned to the racemic and meso conformations of the receptor and have approximately equal intensities. As the temperature is raised incrementally, these two peaks broaden, then coalesce (at 27.5 °C), and at 70 °C a single peak is observed at $-2706\text{ }\delta$ (see Supporting Information). An Eyring plot¹⁹ of the data provides $\Delta G_{20^\circ\text{C}}^\ddagger = 12 \pm 2\text{ kcal mol}^{-1}$ and $\Delta H^\ddagger = 2.7$

kcal mol^{-1} and $\Delta S^\ddagger = -33\text{ cal/(mol K)}$. The receptor, **3**, bears two sites having puckered rings, but inverting the conformational chirality on one ring is sufficient to cause meso–racemic change. Hence, as compared to the conformational inversion of a single ring, the receptor racemic–meso interconversion rate is twice that of a single inversion. Accounting for this statistical factor, $\Delta G_{20^\circ\text{C}}^\ddagger$ becomes 13 kcal mol^{-1} and ΔS^\ddagger is -34 cal/(mol K) , and ΔH^\ddagger , of course, remains the same, 2.7 kcal mol^{-1} .

The conformational interconversion of the receptor, **3**, resembles that of the well-studied molecule 9,10-dihydro-phenanthracene (9,10-DHP).²⁰ The 9,10-DHP molecule is believed to undergo conformational interconversion very rapidly, so that even at $-130\text{ }^\circ\text{C}$ no line broadening of the ¹H NMR spectrum is observed, suggesting an interconversion barrier of less than 7 kcal mol^{-1} . The enthalpy barrier determined for receptor **3** of about 2.7 kcal mol^{-1} is consistent with calculation and experiment.²⁰ The large negative entropy of activation, however, does not elicit a ready explanation. The lifetime of any conformational state of the receptor is very short, about $5 \times 10^{-4}\text{ s}$ at room temperature. Of the three crystal structures obtained for these receptors,^{11,14} all have the receptor in the racemic conformation which may reflect the exigencies of crystal packing, but it appears that both racemic and meso forms exist in solutions. This latter supposition appears to be confirmed by the ¹⁹⁵Pt NMR spectrum of the adduct formed between receptor **3** and [Pt(salap)NH₃] in acetonitrile solutions.

Three signals are observed for 1:1 acetonitrile solutions of receptor and guest at 20 °C; the receptor shows broad signals at $-2669\text{ }\delta$ and $-2736\text{ }\delta$ of similar intensities, and the incarcerated guest provides a signal at $-2534\text{ }\delta$. Upon raising the temperature to 70 °C, we found that the two receptor signals coalesce to a single peak at $-2690\text{ }\delta$, and the guest signal occurs at $-2554\text{ }\delta$. Because of the exceedingly long acquisition times, the temperature profile of the host–guest complex was not pursued. It is clear, however, that racemic–meso interconversion occurs with the host–guest complex.

It was considered possible that ¹⁹⁵Pt NMR spectra might provide a quantitative estimate of the rates of intermolecular exchange between the free and associated guest. Using a 2:1 ratio of guest to host, we found that ¹⁹⁵Pt NMR spectra were recorded up to 80 °C in acetonitrile solutions. No coalescence of the ¹⁹⁵Pt NMR signals of the guest nuclei was observed.

Conclusions

This work has demonstrated that properly designed metal-based receptors can deploy metal–metal interactions with metal-based guests for molecular recognition. The present study appears to be the first example where such interactions have been used in molecular recognition. The work has demonstrated the similarity of the structures in solution and the solid state and has indicated that metal–metal interactions of the kind discussed here can be as large as π – π interactions.

(18) Pregosin, P. S. *Coord. Chem. Rev.* **1982**, *44*, 247–291. Pregosin, P. S. *Annu. Rep. NMR Spectrosc.* **1986**, *17*, 285–349.

(19) Schneider, H. J. *Principles and Methods in Supramolecular Chemistry*; John Wiley & Sons: New York, 2000. Binsch, G. In *Topics in Stereochemistry*; Eliel, E. L., Allinger, N. L., Eds.; Interscience Publishers: New York, 1968; Vol. 3, pp 97–185. Petrucci, S.; Eyring, E. M.; Konya, G. In *Comprehensive Supramolecular Chemistry*; Davies, S. E. D., Ripmeester, J. A., Eds.; Pergamon: Oxford, U.K., 1996; Vol. 8, pp 483–497. Gunther, H. *NMR Spectroscopy*; John Wiley & Sons: Chichester, 1995; pp 335–390.
(20) Gunther, H. *NMR Spectroscopy*; John Wiley & Sons: Chichester, 1995; pp 335–390. Oki, M.; Iwamura, H.; Hayakawa, N. *Bull. Chem. Soc. Jpn.* **1963**, *36*, 1542–1543. Schloegl, K.; Werner, A.; Widhalm, M. *J. Chem. Soc., Perkin Trans. 1* **1983**, 1731–1735.

Experimental Section

General Procedures. All reagents were obtained from commercial suppliers and were generally used without further purification. All reactions were performed under an atmosphere of argon, unless otherwise specified. Electronic absorption spectra were obtained using a Perkin-Elmer Lambda 6 UV/VIS spectrophotometer. Elemental analyses were performed by Desert Analytics, Tucson, AZ. Conductance measurements were performed at 23 °C with 1×10^{-3} M solutions using a YSI Scientific model 35 conductance meter. ^1H and ^{13}C NMR spectra were recorded using a Bruker DRX500 or a Bruker DMX500 Fourier transform spectrometer. ^{195}Pt NMR spectra were recorded using a Bruker DRX400. Proton and carbon chemical shifts, δ , are reported in ppm, referenced to tetramethylsilane (TMS), and platinum chemical shifts, δ , are reported in ppm and referenced to a saturated solution of $\text{K}_2[\text{PtCl}_6]$ in D_2O . Coupling constants, J , are reported in hertz. Melting points are uncorrected. Acetonitrile was dried over CaH_2 , tetrahydrofuran was dried over potassium/benzophenone ketyl, diethyl ether was dried over sodium/benzophenone ketyl, and methylene chloride was dried over CaH_2 . Thin-layer chromatography was carried out using precoated silica gel (Whatman PE SIL G/UV) or precoated aluminum oxide (J. T. Baker, aluminum oxide IB-F). Silica gel 60 Å (Merck, 230–400 mesh) and aluminum oxide 58 Å (either activated, basic, Brockman I or activated, neutral, Brockman I) were used for chromatography as indicated. Celite is J. T. Baker Celite 503. The complex, $[\text{Pt}(\text{salap})\text{DMSO}]$, was prepared by the excellent method of Pregosin,¹⁶ starting from $[\text{Pt}(\text{DMSO})_2\text{Cl}_2]$.²¹ The preparation of the receptor ligand, L_R , has been previously described.¹¹ All other chemicals were purchased from Aldrich Chemical Co. and were used as received.

***n*-Bu₄N[Pt(salap)CN].** A dried 50 mL flask was charged with $[\text{Pt}(\text{salap})\text{DMSO}]$ (0.149 g, 0.307 mmol) dissolved in warm acetonitrile (25 mL). A solution of tetra-*n*-butylammonium cyanide (0.0825 g, 0.307 mmol) in methanol (8 mL) was added to the stirred solution. The reaction was stirred at room temperature for 21 h, during which time the color changed from yellow to orange. The solvent was removed under reduced pressure to yield the crude product as orange needles. The product was dissolved in hot acetonitrile (3 mL), and the solution was allowed to cool. Ether was added to the mixture at a rate of 1 mL every 5 min. Large orange blades of the product (0.265 g, 95.8%) were collected by filtration and washed with ether (5 mL) and pentane (5 mL). ^1H NMR (CD_3CN , 16 °C, 500 MHz): δ 0.908 (t, $J = 7.36$, 12H), 1.29 (m, 8H), 1.54 (m, 8H), 3.04 (m, 8H), 6.62 (m, 1H), 6.71 (m, 1H), 6.95 (dd, $J_1 = 8.31$, $J_2 = 1.37$, 1H), 7.01 (m, 1H), 7.08 (m, 1H), 7.40 (m, 1H), 7.71 (dd, $J_1 = 8.02$, $J_2 = 1.82$, 1H), 7.91 (dd, $J_1 = 8.25$, $J_2 = 1.34$, 1H), 9.02 (s, 1H). ^3J (^{195}Pt , H-9.02) = 32.8 Hz. ^{13}C NMR (CD_3CN , 16 °C, 125 MHz): δ 13.76, 20.24, 24.25, 59.20, 115.63, 116.2, 116.5, 118.7, 119.7, 122.4, 122.6, 129.0, 133.2, 135.2, 139.2, 145.0, 163.2, 170.4. ^{195}Pt NMR (CD_3CN , 16 °C, 86 MHz): δ -2014 (br s). $\Lambda_{\text{M}}(\text{acetone}) = 89 \Omega^{-1} \text{cm}^2 \text{mol}^{-1}$. Anal. Calcd for $\text{C}_{30}\text{H}_{45}\text{N}_3\text{O}_2\text{Pt}$: C, 53.40; H, 6.72; N, 6.23. Found: C, 53.43; H, 6.89; N, 6.29.

***n*-Bu₄N[Pt(salap)Cl].** A dried 50 mL flask was charged with $[\text{Pt}(\text{salap})\text{DMSO}]$ (0.400 g, 0.826 mmol) dissolved in warm acetonitrile (28 mL). Tetra-*n*-butylammonium chloride (0.574 g, 2.06 mmol) was added as a solid to the yellow solution. The solution was refluxed for 5 h, during which time the color gradually changed to red-orange. The solvent was removed under reduced pressure, and the resulting orange solid was slurried with 5% methanol in distilled water (20 mL). The slurry was filtered and was washed with distilled water (5 mL) and 5% methanol in distilled water (5 mL). The solid was dried. The orange powder was dissolved in acetonitrile (10 mL) and was filtered through Celite. The red filtrate was concentrated to ~ 5 mL. Upon being cooled to 0 °C, the product crystallized as an orange solid. Slow addition of ether (10 mL) brought out the remaining crystals. The product was collected by filtration and was washed with ether (5 mL) and pentane (5 mL), yielding orange crystals of the chloro complex (0.550 g, 97.3%).

^1H NMR (CD_3CN , 16 °C, 500 MHz): δ 0.901 (t, $J = 7.36$, 12H), 1.29 (m, 8H), 1.54 (m, 8H), 3.06 (m, 8H), 6.58 (m, 1H), 6.66 (m, 1H), 6.93 (dd, $J_1 = 8.33$, $J_2 = 1.34$, 1H), 6.97–6.99 (m, 2H), 7.41 (m, 1H), 7.73 (dd, $J_1 = 8.02$, $J_2 = 1.82$, 1H), 7.91 (dd, $J_1 = 8.26$, $J_2 = 1.34$, 1H), 9.02 (s, 1H). ^3J (^{195}Pt , H-9.02) = 80.3 Hz. ^{13}C NMR (CD_3CN , 16 °C, 125 MHz): δ 13.8, 20.3, 24.3, 59.2, 115.1, 116.0, 116.4, 118.5, 122.5, 123.4, 128.8, 132.4, 134.4, 141.5, 141.6, 162.6, 170.5. ^{195}Pt NMR (CD_3CN , 16 °C, 86 MHz): δ -1122 (br s). $\Lambda_{\text{M}}(\text{acetone}) = 89 \Omega^{-1} \text{cm}^2 \text{mol}^{-1}$. Anal. Calcd for $\text{C}_{29}\text{H}_{45}\text{ClN}_3\text{O}_2\text{Pt}$: C, 50.91; H, 6.63; N, 4.09. Found: C, 50.73; H, 6.76; N, 4.11.

[Pt(salap)NH₃]. A dried 100 mL sealable flask was charged with $[\text{Pt}(\text{salap})\text{DMSO}]$ (0.750 g, 1.55 mmol) dissolved into freshly distilled CH_3CN (60 mL). Ammonia, as a 7 M solution in methanol (6.60 mL, 46.5 mmol), was added to the yellow solution of the DMSO complex. The reaction flask was sealed, and the reaction was heated to 60 °C using an oil bath. The reaction was stirred at this temperature for 44 h, during which time the color changed to light orange, and the product began to crystallize from the reaction mixture. At the end of this period, the reaction mixture was permitted to cool and was transferred to a 200 mL flask. The ammonia was removed under reduced pressure, and the volume was made up to 75 mL by the addition of CH_3CN . The ammine complex was dissolved by heating the mixture. Upon being cooled to -25 °C, the product crystallizes as small, orange needles. The needles (0.564 g, 86.0%) were collected by filtration and were washed with cold CH_3CN (3 mL), ether (5 mL), and pentane (5 mL). Solutions of the ammine complex in THF must be handled under an atmosphere of argon. Solutions of the ammine complex in acetonitrile, however, are stable in air. ^1H NMR (CD_3CN , 16 °C, 500 MHz): δ 3.88 (s, 3H), 6.65 (m, 1H), 6.76 (m, 1H), 6.94 (dd, $J_1 = 8.33$, $J_2 = 1.16$, 1H), 7.02–7.08 (m, 2H), 7.46 (m, 1H), 7.77 (dd, $J_1 = 8.05$, $J_2 = 1.79$, 1H), 7.93 (dd, $J_1 = 6.75$, $J_2 = 1.31$, 1H), 8.94 (s, 1H). ^3J (^{195}Pt , H-9.02) = 71.1 Hz. ^{13}C NMR ($\text{DMF}-d_7$, 16 °C, 125 MHz): δ 115.1, 116.26, 116.29, 118.1, 121.8, 123.5, 128.6, 132.5, 134.7, 140.8, 143.4, 162.3, 169.9. ^{195}Pt NMR ($\text{DMF}-d_7$, 16 °C, 86 MHz): δ -1517 (br s). $\Lambda_{\text{M}}(\text{acetone}) = 0.41 \Omega^{-1} \text{cm}^2 \text{mol}^{-1}$. Anal. Calcd for $\text{C}_{13}\text{H}_{12}\text{N}_2\text{O}_2\text{Pt}$: C, 36.88; H, 2.86; N, 6.62. Found: C, 36.77; H, 2.85; N, 6.57.

[L_RPtCl₂](SbF₆)₂ (3). The following procedure must be performed with rigorous exclusion of water. A dried 25 mL flask was charged with AgSbF_6 (0.150 g, 0.437 mmol) dissolved in anhydrous acetone (5 mL). A suspension of $[(\text{COD})\text{PtCl}_2]$ (0.121 g, 0.218 mmol) in dry acetone (3 mL) was added to the colorless solution of the silver salt. Upon addition, the COD complex rapidly dissolved, and AgI was precipitated. The reaction was stirred for 30 min at room temperature, with brief sonication midway through this period. The mixture was filtered through a dried, fine frit into a dry 50 mL flask. A small amount of acetone was used to wash the collected AgI . The receptor ligand, L_R (0.102 g, 0.1091 mmol), was added to the pale yellow solution of the platinum complex in acetone. The receptor ligand dissolved rapidly, and the color changed to golden yellow. The reaction was stirred at room temperature for 22 h. Tetra-*n*-butylammonium chloride (0.067 g, 0.2401 mmol) was added as a solution in dry acetone (5 mL). The reaction was stirred at room temperature for 40 min, during which time the color lightened and a precipitate began to form. Anhydrous methanol (15 mL) was added, dissolving nearly all of the material, and the reaction was heated to boiling. The acetone and all but 5 mL of the methanol were permitted to evaporate from the flask, causing the product to form as a fine, yellow solid. The mixture was cooled to 0 °C and was filtered. The yellow solid (0.197 g, 96.4%) was collected and was washed with cold methanol (5 mL), ether (10 mL), and pentane (10 mL). ^1H NMR (CD_3CN , 60 °C, 500 MHz): δ 1.45 (s, 18H), 2.89 (t, $J = 6.55$, 4H), 3.07 (t, $J = 6.36$, 4H), 7.19 (m, 4H), 7.22 (d, $J = 1.79$, 2H), 7.63 (d, $J = 7.64$, 2H), 7.66 (t, $J = 1.79$, 1H), 7.82 (dd, $J_1 = 7.60$, $J_2 = 1.79$, 2H), 7.91–7.97 (m, 12H), 8.27 (s, 4H), 9.02 (d, $J = 1.82$, 2H). ^{195}Pt NMR (CD_3CN , 75 °C, 86 MHz): δ -2702 (br s). $\Lambda_{\text{M}}(\text{acetonitrile}) = 219 \Omega^{-1} \text{cm}^2 \text{mol}^{-1}$. Anal. Calcd for $\text{C}_{65}\text{H}_{55}\text{Cl}_2\text{F}_{12}\text{N}_7\text{Pt}_2\text{Sb}_2$: C, 41.82; H, 2.97; N, 3.80. Found: C, 41.77; H, 2.95; N, 3.75.

(21) Romeo, R.; Scolaro, L. M. *Inorg. Synth.* **1998**, *32*, 153–158.

Host–Guest Interaction of $[\text{L}_R\text{Pt}_2\text{Cl}_2](\text{SbF}_6)_2$ with $[\text{Pt}(\text{salap})\text{NH}_3]$. A series of 1.00 mM solutions of $[\text{L}_R\text{Pt}_2\text{Cl}_2](\text{SbF}_6)_2$ in CD_3CN containing varying amounts of $[\text{Pt}(\text{salap})\text{NH}_3]$, ranging from 0.326 to 2.35 mM, was prepared and was examined by ^1H NMR. The host in CD_3CN solution is yellow, as is the guest. The host–guest mixtures vary in color from pale orange to deep red. The mole ratio method was applied, and the stoichiometry of the association was found to be 1:1 (Supporting Information). The maximum chemical shift change for any proton of the host was 0.9 ppm (H_g). Several other protons of the host had maximum changes of approximately 0.25–0.6 ppm. The maximum chemical shift change observed for the guest was 1.1 ppm (for proton H_p), with several other chemical shifts changing by about 0.4–1.0 ppm. The association constant, K , was found to be large from the stoichiometry determination data, so a series of more dilute solutions was prepared to more accurately determine K . A series of solutions containing 0.100 mM $[\text{L}_R\text{Pt}_2\text{Cl}_2](\text{SbF}_6)_2$ and the guest concentrations, varying in concentration from 0.0588 to 0.176 mM, was prepared and was examined by ^1H NMR. The data were analyzed using a curve fitting procedure, and K was found to be $51\,000 \pm 8400 \text{ M}^{-1}$ for both concentration sets.

Host–Guest Interaction of $[\text{L}_R\text{Pd}_2\text{Cl}_2](\text{SbF}_6)_2$ with $[\text{Pt}(\text{salap})\text{NH}_3]$. A series of 1.00 mM solutions of $[\text{L}_R\text{Pd}_2\text{Cl}_2](\text{PF}_6)_2$ in CD_3CN containing varying amounts of $[\text{Pt}(\text{salap})\text{NH}_3]$, ranging from 0.181 to 5.05 mM, was prepared and was examined by ^1H NMR. The host in CD_3CN solution is yellow, as is the guest. The host–guest mixtures vary in color from pale orange to red-orange. The mole ratio method was applied, and the stoichiometry of the association was found to be 1:1 (Supporting Information). The maximum chemical shift change for any proton of the host was 0.75 ppm (H_g). Several other protons of the host had maximum changes of approximately 0.25–0.6 ppm. The maximum chemical shift change observed for the guest was 1.27 ppm (H_p), with several other chemical shifts changing by about 0.4–1.1 ppm. Once again, the association constant, K , was found to be large, so a series of more dilute solutions was prepared. A series of solutions containing 0.100 mM $[\text{L}_R\text{Pd}_2\text{Cl}_2](\text{PF}_6)_2$ with the guest, varying in concentration from 0.0577 to 0.143 mM, was prepared and was examined by ^1H NMR. The data were analyzed using a curve fitting procedure, and K was found to be $12\,000 \pm 2900 \text{ M}^{-1}$ for both concentration sets.

Crystallographic Structural Determination for $[\text{L}_R\text{Pt}_2\text{Cl}_2]\cdot[\text{Pt}(\text{salap})\text{NH}_3]\cdot(\text{SbF}_6)_2\cdot(\text{CH}_3\text{CH}_2\text{CN})$. Crystals of the complex were grown by dissolving a 1:1 mixture of the host and guest in propionitrile and vapor diffusing with methanol for 6 days.

Data Collection. A needle-shaped crystal ($0.08 \times 0.005 \times 0.005$ mm) was selected under a polarizing microscope while immersed in Fluorolube oil to avoid possible loss of solvent of crystallization. The crystal was removed from the oil using a tapered glass fiber that also served to hold the crystal for data collection. The crystal was mounted and centered on a goniometer with Kappa geometry at ChemMatCARS Sector 15 beamline at the Advanced Photon Source at the Argonne National Laboratory. The sample was cooled to 110 K. Still images

showed the diffractions to be sharp. Data collection consisted of 720 frames separated by 0.5° rotations in ϕ with the detector to sample distance set to 9 cm. The integration time for each frame was 2 s. The crystallographic information is summarized in Table 1 of the Supporting Information, and a CIF file is supplied as Supporting Information.

The unit cell was obtained using SMART, and integration of intensities and refinement of cell parameters were done using SAINT.²² Absorption corrections were applied using SADABS²² based on redundant diffractions.

Structure Solution and Refinement. The space group was determined as $P\bar{1}$ on the basis of systematic absences and intensity statistics. Patterson methods were used to locate the Pt atoms as well as Sb and F atoms. Repeated difference Fourier maps allowed recognition of all expected C, N, O, and Cl atoms. Hydrogen atom positions were calculated. Final refinement was anisotropic for all non-hydrogen atoms and isotropic for H atoms. No anomalous bond lengths were noted, although a number of displacement ellipsoids were elongated possibly due to disorder in the *tert*-butyl groups.

Acknowledgment. This work was supported by the Department of Energy, Basic Sciences Division. The authors thank Paul Pregosin for advice on the complexities of ^{195}Pt NMR spectra, and the Argonne National Laboratories are thanked for access to the CARS facility. ChemMatCARS Sector 15 is principally supported by the National Science Foundation/Department of Energy under grant numbers CHE9522232 and CHE0087817 and by the Illinois board of higher education. The Advanced Photon Source is supported by the U.S. Department of Energy, Basic Energy Sciences, Office of Science, under Contract No. W-31-109-Eng-38.

Supporting Information Available: A CIF file of $3\cdot[\text{Pt}(\text{salap})\text{NH}_3]\cdot(\text{SbF}_6)_2\cdot(\text{CH}_3\text{CH}_2\text{CN})$ structure determination, additional views of the crystal structure $3\cdot[\text{Pt}(\text{salap})\text{NH}_3]\cdot(\text{SbF}_6)_2\cdot(\text{CH}_3\text{CH}_2\text{CN})$, a diagram showing the interplanar separations and angles found in the crystal structure of $3\cdot[\text{Pt}(\text{salap})\text{NH}_3]\cdot(\text{SbF}_6)_2\cdot(\text{CH}_3\text{CH}_2\text{CN})$, ^1H NMR and NOESY spectra of 1:1 host:guest solutions of $3(\text{SbF}_6)_2$ with $[\text{Pt}(\text{salap})\text{NH}_3]$ and $1(\text{PF}_6)_2$ with $[\text{Pt}(\text{salap})\text{NH}_3]$, variable temperature ^{195}Pt NMR spectra for $3(\text{SbF}_6)_2$, ^{195}Pt NMR spectra for 1:1 and 1:2 solutions of $3(\text{SbF}_6)_2$ and $[\text{Pt}(\text{salap})\text{NH}_3]$, ^1H NMR titration curves for $1(\text{PF}_6)_2$ with $[\text{Pt}(\text{salap})\text{NH}_3]$ and $3(\text{SbF}_6)_2$ with $[\text{Pt}(\text{salap})\text{NH}_3]$, and absorption spectra for host–guest solutions of $1(\text{PF}_6)_2$ with $[\text{Pt}(\text{salap})\text{NH}_3]$ (PDF). This material is available free of charge via the Internet at <http://pubs.acs.org>.

JA028910Z

(22) Sheldrick, G. *SHELXTL* (version 6.1) program library; G. Bruker Analytical X-ray Systems, Madison, WI, 2000.